Structural Investigation of a Bicelle/Pluronic System by Small Angle Neutron Scattering

R. Soong,[1] P. M. MacDonald,[1] E. Nicholson,[2] M-P. Nieh,[3] J. Katsaras[3]

[1] Department of Chemical and Physical Science, University of Toronto Mississauga, 3359 Mississauga Road North, Mississauga, Ontario, Canada L5L 1C6

[2] Division of Engineering Science, University of Toronto 40 St. George Street, Toronto, Ontario, Canada M5S 2E4

[3] Canadian Neutron Beam Centre, National Research Council Canada, Chalk River Laboratories, Chalk River, ON, Canada K0J 1J0

Bicelles are a model membrane system consisting of binary mixtures of long chain lipids, e.g.,1,2-dimyristoyl-*sn*-glycero-3-phosphocholine (DMPC) and short chain lipids, e.g., 1,2-dihexanoyl-*sn*-glycero-3-phosphocholine (DHPC). Depending on the molar ratio of long to short chain lipids, Q (i.e., [DMPC]/[DHPC]) and temperature, the mixtures can self-assemble into a variety of macroscopic morphologies which include single bilayer discs, chiral nematic ribbons and lamellar sheets perforated with toroidal holes. Importantly for NMR studies, bicelles spontaneously align in magnetic fields such that there is a narrow distribution of orientations of the bilayer normal with respect to the magnetic field.

The Pluronic family of tri-block copolymers consists of a hydrophobic polypropylene oxide (PPO) central block flanked by hydrophilic polyethylene oxide (PEO) end blocks. Pluronics have received particular attention of late because in addition to their potential as drug delivery vehicles and their utility in encouraging drug uptake *in vitro* [1] – [2], they incorporate readily into lipid bilayers where they facilitate lipid flip-flop and transbilayer drug permeation [3] – [4]. We report of a SANS study on bicelle mixtures of zwitterionic DMPC/DHPC/Pluronic as a function of temperature in order to understand the structural transformation of the system.

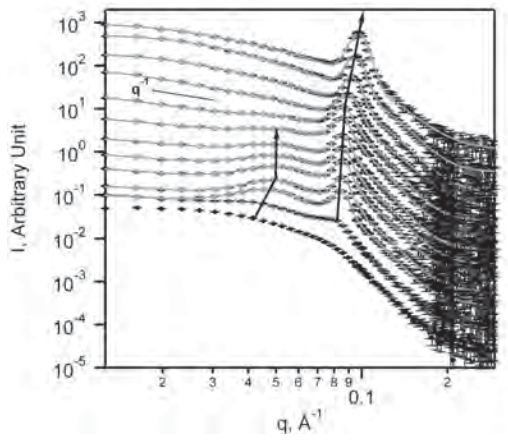

Fig 1. *SANS results of DMPC/DHPC/F68 in D2O (total lipid concentration = 20 wt.%) at a series of temperatures (i.e., 294.5, 298.5, 300, 301.9, 303.5, 305, 306.7, 308, 309.7, 311.2, 312.8, 314.4 and 318.6 K, from bottom to top). The data were rescaled for clarity. The solid symbols are data from the discoidal micellar phase and the gray lines are the best-fits to the data using Equation 1. The two lines show the movement of the two quasi-Bragg peaks as a function of temperature.*

DMPC, DHPC and DMPG were purchased from Avanti Polar Lipids. Pluronic F68 was purchased from Sigma-Aldrich. The samples were prepared in D_2O with Q = 4.5 and 0.4 mol% of Pluronic at three total lipid concentrations, c_{lp} of 20, 25 and 30 wt.%. SANS experiments were conducted at the N5 triple-axis neutron spectrometer [5]. The wavelength of the neutrons, λ was chosen to be 2.37 Å by a pyrolytic graphite monochromator. The raw scattering intensities were corrected using sample and empty transmission cell measurements. SANS data are presented as a function of the scattering vector, q, defined as $(4\pi/\lambda)\sin(\theta/2)$, where θ is the scattering angle.

The SANS data obtained from all three samples (c_{lp} = 20. 25 30 wt.%) show the same structural transition and temperature dependence, as a result only the SANS data from the c_{lp} = 20 wt.% sample (Fig 1) is reported. At 295 K SANS intensities (Figure 1) at low q remain constant, but monotonically decay at higher q in a manner reminiscent of bicelles [6] – [8]. At higher temperatures, a phase transition is observed, where the scattering pattern transforms into two quasi-Bragg peaks sitting on two decaying backgrounds with slopes, -n and -m, which can be best-fit using a phenomenological equation (Equation 1) to obtain the peak positions (q_{p1} and q_{p2}) and their corresponding peak widths (σ_{qp1} and σ_{qp2}). The equation is written as follows:

$$\frac{s_o}{\left(1+s_1\cdot q^{m}+s_2\cdot q^{n}\right)}+p_1\cdot e^{\frac{(q-q_1)^2}{\sigma_{q1}^2}}+p_2\cdot e^{\frac{(q-q_2)^2}{\sigma_{q2}^2}}+BDG, \quad (1)$$

where s_0, s_1, s_2, p_1, p_2 are coefficients giving the relative ratio of the background scattering and amplitude of each Gaussian peak. The fact that at 298.5 K the two peaks are found simultaneously at $q_{p1} \sim 0.04$ and $q_{p2} \sim 0.08$ Å^{-1}, with the width of the low q peak σ_{qp1} being approximately ten times broader than the one at high q, implies that the two peaks are possibly originating from in-plane (broad peak) and out-of-plane (sharp peak) structures of the lamellar morphology [9]. These two peaks are most evident between 300K and 303K, and persist until 308 K. As the temperature is increased beyond 310 K, only the sharp peak is observed at ~ 0.095 Å^{-1} (i.e., the in-plane structure has been destroyed), a repeat spacing usually associated with pure DMPC multilamellar vesicles (MLV) [6] – [8], [10] – [11]. It should be noted that the morphology between 298.5 K and 308 K exhibits the strongest susceptibility to magnetic alignment, where structures have been proposed to be either bilayered ribbons [8], [10] – [11] or perforated lamellae [7] – [12]. The best fit results from all three samples, as a function of temperature, are summarized in Table 1 (shown on next page).

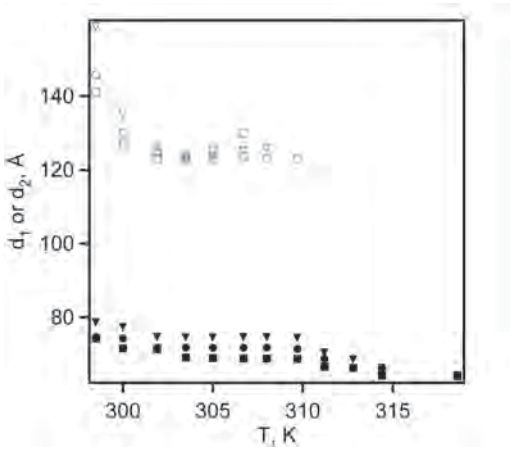

Fig 2. *The values of d-spacing as determined from SANS data of 30 wt.% (circles), 25 wt.% (squares), 20 wt.% (triangles). The solid symbols represent the lamellar spacings, while the open symbols represent spacings between the ribbons.*

Figure 2 shows that the characteristic length d_1 (calculated from $2\pi/q_{p1}$) is plotted as a function of T. The value of d1 drops from 298.5 K to 300 K, and remains approximately constant between 300 K and 308 K. The fact that the σ_{qp1} values are relatively large (0.009 ~ 0.014 Å^{-1}) indicates that the variations in d_1 are rather significant. For this range of temperatures, a ribbon-like morphology has previously been reported [8], [10] – [12]. It is thus reasonable to assume that the in-plane characteristic length is arising from the average spacing between individual ribbons. If this is the case, it also makes sense that the correlation length should be small, giving rise to a broad peak quasi Bragg peak. Evidence for the ribbon morphology is that the slope at low q decays as q^{-1}, a feature characteristic of long one-dimensional objects. For homogeneously dispersed ribbons, d_1 is expected to scale as (lipid concentration)$^{-1/2}$, the result of two-dimensional swelling. However, in Figure 2 d_1 does not change as a function of lipid concentration, indicating that the ribbons do not freely swell, but that they are somehow inter-connected. As temperature increases beyond 308 K, the peak associated with the correlation between ribbons disappears, while the q^{-1} decay remains unaltered, indicating that although the ribbons are still present, they are no longer correlated.

The high q sharp peak (σ_{qp2} ranged from 0.001 to 0.002 Å^{-1}) represents a smectic phase, similar to the lamellar phase previously reported [8] – [13]. Between 300 K and 310 K, the repeat spacing, ($2\pi/q_{p2}$) exhibits no temperature dependence (d_2 > 68 Å), and then drops to the nominal value of 64 Å (the lamellar spacing of pure DMPC MLVs in water [14]) for all samples above 314 K (Figure 2). The appearance of the samples also turns cloudy, typical of MLVs at temperatures ≥ 314 K. The variation of the assumed lamellar spacing d_2 suggests that the intermediate temperature phase, which is also magnetically alignable, should be different from MLVs that do not magnetically align. Figure 2 also shows that, unlike lamellae doped with a charged lipid [6] – [7], where the lamellar spacing increases linearly with decreasing lipid concentration, the swelling ability of this magnetically alignable phase seems somewhat limited when diluted from 30 to 20 wt.%, swelling only a few Ångstroms (i.e., between 68 Å and 75 Å). This behaviour is consistent with that observed in long-chain zwitterionic phospholipid bilayers [15] – [16].

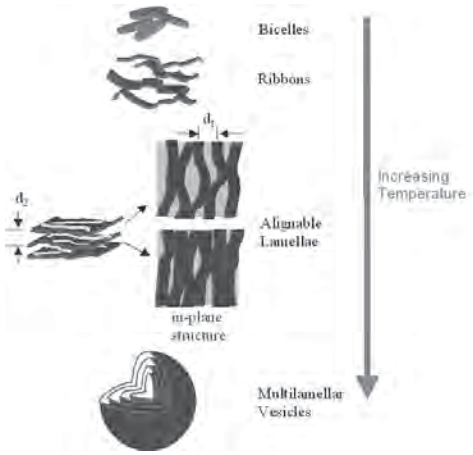

Fig 3. *A schematic of structural transformation of the zwitterionic (DMPC/DHPc/F68) mixtures upon variation of T.*

In light of the aforementioned analysis, we propose the coexistence of ribbons and lamellae as the magnetically alignable phase. The question is whether or not they are two independent, but coexisting morphologies. The simultaneous appearance of the two quasi-Bragg peaks and the fact that these quasi-Bragg peaks do not change much with swelling, implies that the ribbons and the lamellae are part of the same morphology. Figure 3 schematically illustrates the various morphologies that are formed as a function of temperature. As previously reported [6] – [7], with increasing temperature low temperature bicelles composed of DMPC and DHPC coalesce into worm-like ribbons due to the increased line tension resulting from the loss of DHPC into solution from the edge of the bilayered micelle. At this stage, the ribbons are not strongly correlated with each other i.e., no correlation length between individual ribbons is observed. However, as the temperature is increased, approaching the main transition temperature of DMPC (~ 296 K), DHPC becomes miscible with DMPC, as both lipids are now in the liquid crystalline (L_α) phase. This results in a further loss of DHPC from the ribbon's edge, this time to the ribbon's DMPC-rich planar region. The ribbon's edge becomes unstable causing individual ribbons to partially fuse, forming extended lamellar sheets, while in places maintaining the ribbon morphology (Figure 3). The ribbon spacing (d_1) decreases, while the association between ribbons becomes more significant as a result of being confined within a lamellar sheet, (a broad peak). Interestingly, ribbon spacing is not affected by lipid concentration. In fact, the cryo-transmission electron microscopy (cryo-TEM) images reported by van Dam *et al.*[12] illustrated a similar ribbon spacing (100 ~ 150 Å) for [DMPC]/[DHPC] ratios of between 2.5 and 4, and at a much lower lipid concentration (3 wt.%). Finally, the fact that the samples turn translucent implies that the ribbon aggregate lamellar morphology has dimensions of the order of visible light. Increasing the temperature further results in the sample

becoming opaque, indicating the formation of MLVs as a result of the DHPC now leaving the lamellae.

Table 1. The best fit results of quasi-Bragg peak positions and their associated widths from 20, 25 and 30 wt.% DMPC/DHPC/F68 (zwitterionic) solutions (the uncertainties of peak positions and peak widths associated with inter ribbon correlations are less than ±0.003 and ±0.002, respectively; for lamellar correlation lengths these values are less than ±0.002 and ±0.0005, respectively)

T, K	zwitterionic					
	20 wt.%		25 wt.%		30 wt.%	
	q_{p1} $\sigma_{q_{p1}}$	q_{p2} $\sigma_{q_{p2}}$	q_{p1} $\sigma_{q_{p1}}$	q_{p2} $\sigma_{q_{p2}}$	q_{p1} $\sigma_{q_{p1}}$	q_{p2} $\sigma_{q_{p2}}$
298.5	0.040 0.009	0.080 0.0037	0.044 0.019	0.084 0.0017	0.043 0.008	0.084 0.0015
300	0.047 0.011	0.081 0.0012	0.049 0.018	0.088 0.0014	0.048 0.012	0.085 0.0012
301.9	0.050 0.012	0.084 0.0012	0.051 0.017	0.088 0.0013	0.050 0.018	0.087 0.0014
303.5	0.051 0.013	0.084 0.0012	0.051 0.024	0.088 0.0013	0.051 0.019	0.088 0.0014
305	0.051 0.014	0.084 0.0012	0.050 0.026	0.091 0.0014	0.051 0.020	0.088 0.0015
306.7	0.050 0.012	0.084 0.0013	0.048 0.029	0.091 0.0014	0.051 0.022	0.088 0.0015
308	0.050 0.010	0.084 0.0013	—	0.091 0.0013	0.051 0.023	0.088 0.0016
309.7	—	0.084 0.0014	—	0.091 0.0013	0.051 0.017	0.088 0.0015
311.2	—	0.089 0.0024	—	0.094 0.0013	—	0.091 0.0014
312.8	—	0.092 0.0013	—	0.095 0.0013	—	0.095 0.0014
314.4	—	0.095 0.0014	—	0.098 0.0011	—	0.095 0.0014
318.6	—	0.098 0.0014	—	0.098 0.0011	—	0.098 0.0014

References

[1] Kabanov, A.V.; Batrakova, E.V.; Alakhov, V.Y. Adv. Drug Deliv. Rev. 2002, 54, 759-779.

[2] Kabanov, A.V. Batrakova, E.V.; Miller, D.W. Adv. Drug Deliv. Rev. 2003, 55, 151-164 2003.

[3] Yaroslavov, A. A.; Melk-Nubarov, N. S.; Menger, F. M. Acc. Chem. Res. 2006, 39, 702-710.

[4] Demina, T.; Grozdova, I.; Krylova, O.; Zhirnov, A.; Istratov, V.; Frey, H.; Kautz, H.; Melik-Ŋubarov, N. Biochem. 2005, 44, 4042-4054.

[5] Nieh, M.-P.; Yamani, Z.; Kucerka, N.; Katsaras, J.; Burgess, D.; Breton, H. Rev. Sci. Instrum. 2008, 79, 095102.

[6] Nieh, M.-P.; Glinka, C. J.; Krueger, S.; Prosser, R. S.; Katsaras, J. Langmuir. 2001, 17, 2629-2638.

[7] Nieh, M.-P.; Glinka, C. J.; Krueger, S.; Prosser, R. S.; Katsaras, J. Biophy. J. 2002, 82, 2487-2498.

[8] Katsaras, J.; Harroun, T. A.; Pencer, J.; Nieh, M.-P. Naturwissenschaften. 2005, 92, 355–366.

[9] Katsaras, J.; Raghunathan,V. A.; Dufourc, E. J.; Dufourcq, J. 1995 Biochemistry. 34, 4684-4688.

[10] Nieh, M.-P.; Raghunathan, V. A.; Glinka, C. J.; Harroun, T. A.; Pabst, G.; Katsaras, J. Langmuir. 2004, 20, 7893-7897.

[11] Harroun, T. A.; Koslowsky, M.; Nieh, M.-P.; de Lannoy, C.-F.; Raghunathan, V. A.; Katsaras, J. Langmuir. 2005, 21, 5356-5361.

[12] van Dam, L.; Karlsson, G.; Edwards, K. Biochim. Biophys. Acta –Biomembranes. 2004, 1664, 241– 256.

[13] van Dam, L.; Karlsson, G.; Edwards K. Langmuir, 2006, 22, 3280-3285. Kučerka, N; Nieh, M.-P.; Pencer, J.; Harroun, T. A.; Katsaras, J. Curr. Opin. Colloid Interf. Sci. 2007, 12, 17–22.

[14] Katsaras, J. and Stinson, R. H. Biophy. J. 1990, 57, 649-655.

[15] Katsaras, J. J. Phys. Chem. 1995, 99, 4141-4147.